Modeling the Spread of Influenza Among Cities *

James M. Hyman
Theoretical Division, MS-B284
Center for Nonlinear Studies
Los Alamos National Laboratory
Los Alamos, NM 87545
Tara LaForce
Computational and Applied Mathematics Program
University of Texas at Austin
Austin, Texas 78712

May 2, 2003

Abstract

We develop a differential equation model for the spread of influenza through a network of isolated population centers with limited migration among them. The epidemic model is applied to help better understand the spread of influenza among 33 major cities in the United States. We estimate the basic epidemiological parameters for a simple Susceptible, Infected, Recovered (SIR) model within each city by combining data from the influenza transmission studies, the reported mortality data attributed to influenza and pneumonia, and a least squares fit of the observed seasonal variation in the number of influenza cases. The epidemic model is formulated on a discrete network with the cities at the nodes and the bonds between the nodes representing movement of people between the cities. The nodes are weighted by the population of the city it is identified with. We use data for the airline passengers flying between the cities each day to approximate the number of people moving between the cities. The SIR network model captures the essential features of the yearly influenza epidemic estimated by Centers for Disease Control (CDC) and Prevention influenza and pneumonia mortality data. The model is used to predict the initial spread of a new infectious agent, such as a new strain of influenza or the severe acute respiratory syndrome (SARS), after it first appears in one of the cities. We apply sensitivity analysis to identify which parameters the model predictions are sensitive to. The numerical simulations demonstrate that the approach has promise in predicting the spread of an infectious agent spreading through a network of cities connected by a highly mobile transportation system.

*This research was supported by the Department of Energy under contracts W-7405-ENG-36 and the National Infrastructure Simulation and Analysis Center (NISAC).

1 Introduction

Every year influenza kills thousands of Americans and millions are stricken ill. Despite attempts to vaccinate high-risk populations the cost of influenza in terms of lost life and lost productivity is still high. Mathematical models can provide insight into how influenza spreads between individual people within a community and across the United States. This insight can potentially help guide health care workers anticipate the number of influenza cases each year and identify anomalies that might foretell an unexpected new or stronger epidemic.

Weekly data on the mortality and morbidity attributed to influenza and pneumonia (P/I) is collected by the Center for Disease Control and Preventions (CDC) Epidemiology Branch Office for each of 122 cities in the United States. We analyze this data search for correlations between the number of cases in a city and other epidemiological parameters, such as the population of the city, the infectiousness of the disease, and the transmission from city to city during an epidemic. We also searched for possible precursor cities that might herald the start of a new season.

The simplest Susceptible-Infected-Recovered (SIR) model, developed in 1927 by Kermack and McKendrick [9] assumes random mixing of the population. Models for the initial spread of infectious agents through nonrandom mixing populations where people move between groups in a single population is needed to predict the early spread of a disease [13]. However, after the short initial growth of an epidemic in a city, the random mixing assumption can be used for the spread of diseases, such as influenza, within a city.

The mixing between the cites still needs to be modeled to predict the spread of a disease between cities when their populations are unevenly spread over a large geographic area. In the 1985, Rvachev and Longini published the first of a series of papers modeling the spread of influenza from city to city around the world during the 1968-1969 pandemic[8] [12]. They developed a multi-city model in which air-travel was used to approximate the spread of the pandemic from its (assumed) origins in Hong Kong to 51 other major populations centers worldwide. The structure of our model is similar to the one developed by Longini and Rvachev.

We model the spread of the disease in each city by a system of deterministic differential equations. The susceptible and infected people are assumed to mix randomly within a city. We assume that the nonrandom mixing of the population among the cities between the major cities is captured in the model by the air travel. We also assume that people continue to travel when they are infectious. This assumption restricts the current model to specific diseases, such as influenza, where people are asymptomatic or only mildly ill while infected. Our model could be extended to account for people who change their travel plans due to the severity of the disease by adding another infection stage in the model.

The model parameters for the transmission and disease progression are estimated from the literature [14][1]. The rate that people move between the cities is based on airline data, as was done in [12]. We were unable to estimate two parameters from the literature, the average number of contacts a typical city person has during a day that could result in transmitting the disease, and the seasonal change in the infectivity of influenza. We assumed that these two parameters were the same for every city and estimated them by a least squares fit to the CDC data. We fit the parameters on several different cities. The fits on the cities with the best data provided similar estimates for these parameter values.

After defining the model and parameters, we compare the results of the model with the data collected by the 122 Cities Mortality Reporting System and reported to the CDC and conclude that this model approximates the magnitude and fluctuation of the influenza seasons for 1996-2001. This simple model did remarkably well at predicting the yearly influenza epidemic.

The SIR transmission model for a single city is then extended to predict the spread of the virus among multiple cities. We provide details on how we estimated the model parameters and data for the population and traffic between the cities. We provide a simple analysis for the reproductive number and the sensitivity of the model predictions to small changes in the parameter estimates. Finally, we provide a comparison of the model predictions with the CDC data for several representative cities.

2 MultiCity Transmission

We first define and analyze the single city model, then add a term to account for the return to susceptibility of an infected person and an emigration/migration term. Next, we generalize the model to a multi-city transmission model where the epidemic is spread through the network of cities by the migration of infected people.

2.1 Single City Transmission Model

By dividing a fixed population into susceptible(S), infected(I) and recovered(R) individuals, the simple SIR model

$$\begin{aligned} dS/dt &= -\lambda S && \text{(1a)} \\ dI/dt &= \lambda S - \alpha I && \text{(1b)} \\ dR/dt &= \alpha I && \text{(1c)} \end{aligned}$$

can predict the spread of the single outbreak of a disease. Here the susceptible population is infected at a rate $\lambda > 0$, and the infected population recovers from illness at the rate $\alpha > 0$. For a randomly mixing population, the infection rate, λ can be estimated by the product of three terms

$$\lambda = r\beta \frac{I}{N} \tag{2}$$

.

The average number of contacts per individual per unit time, $r > 0$, is assumed to be constant for large populations. A contact is defined as an encounter between people that could transmit the disease. When defining r, we have assumed the contacts in the population are random and that the number of contacts per unit time is independent of the population size. This is an appropriate assumption for large cities, but for smaller populations or villages it might be more appropriate for r to be proportional to the total population, $N = S+I+R$, of the city. That is, if the population of the village increased by 10%, then a typical person would have 10% more contacts. This is not true for large cities.

The next factor in λ accounts for the probability of transmitting the disease in a contact. This factor, $\beta > 0$, is proportional to the average infectiousness of an infected person times the average susceptibility of a susceptible person. Influenza is more likely to spread in the winter than the summer. [17, 19, 18, 20] This may be caused by an increased infectiousness of the disease, an increased susceptibility of people, or an increased number contacts with others that might result in transmitting the infection during the winter. For example, people may spend more time indoors. Because r and β only occur as a product in the model, we can approximate both of these effects by allowing the product $r\beta$ to vary through the year.

$$r\beta = \hat{\beta}\hat{r}[1 + \epsilon \sin(2\pi t/365)] \tag{3}$$

Here $\epsilon < 1$ is the fluctuation in infectivity between seasons and will be determined by a fitting ϵ, the seasonal variation of the model to CDC influenza data. We assume that ϵ is the same in all of the cities.

The final factor (I/N) in λ reflects that the probability a randomly chosen contact infected is equal to the fraction of the population that is infected.

2.2 Loss of Immunity

Once entering the recovered state, people slowly return to being susceptible to the currently circulating strain of the virus. This can happen because the small mutations in genetic code in the surface antigens allow influenza to drift in ways that eventually allow it to evade the immune system defenses from an earlier infection. We partially account for the loss of immunity by including a new state between the recovered state and the susceptible state in which people have partial immunity to the current strain of the disease. We define the constant rates η^R for return to partial immunity and η^P for a full return to susceptibility. We include the state by modifying the SIR model, $S \to I \to R$, to an SIRP model, $S \to I \to R \to P \to S$, where P is the stage of partial immunity. To fully account for the drift of the virus requires a multistrain model, and is beyond the scope of this study.

We also extend the model to account for people entering and leaving the population either through birth/death or by leaving the network of cities in the model. We define the migration term in a form where S^0 is the stable susceptible population in the absence of infection. In this simple model, we do not explicitly include a term to account for the increase in mortality due to influenza.

The resulting single city transmission SIPR model is

$$\begin{aligned}
dS/dt &= -\lambda^S S + \eta^P P + \mu(S^0 - S) && \text{(4a)}\\
dI/dt &= \lambda^S S + \lambda^P P - \alpha I - \mu I && \text{(4b)}\\
dR/dt &= \alpha I - \eta^R R - \mu R && \text{(4c)}\\
dP/dt &= \eta^R R - \eta^P P - \lambda^P P - \mu P && \text{(4d)}
\end{aligned}$$

Both susceptible and partially immune people can be infected. As before, the infection rate the fully susceptible population is $\lambda^S = \beta^S r(I/N)$, where β^S is the susceptibility of a person in S. Similarly, partially immune people are infected with the rate $\lambda^P = \beta^P r(I/N)$. Because people in the partially immune state are less likely to be infected in a single contact we assume $\beta^S > \beta^P$. The total population is now defined as $N = S + I + R + P$.

2.3 Multi-city Transmission Model

We begin by modeling two cities (city 1 and city 2) with people traveling between them. The epidemic is modeled within each city by the single city model. We use subscripts to indicate the city number and define m_{ij} to be the number of people traveling from city i to city j per unit time. The equations for city 1 and city 2 are:

$$\begin{aligned}
dS_1/dt &= -\lambda_1^S S_1 + \eta^P P_1 + \mu(S_1^0 - S_1) + m_{21} S_2/N_2 - m_{12} S_1/N_1 && \text{(5a)}\\
dI_1/dt &= \lambda_1^S S_1 + \lambda_1^P P_1 - \alpha I_1 - \mu I_1 + m_{21} I_2/N_2 - m_{12} I_1/N_1 && \text{(5b)}\\
dR_1/dt &= \alpha I_1 - \eta^R R_1 - \mu R_1 + m_{21} R_2/N_2 - m_{12} R_1/N_1 && \text{(5c)}\\
dP_1/dt &= \eta^R R_1 - \eta^P P_1 - \lambda_1^P P_1 - \mu P_1 + m_{21} P_2/N_2 - m_{12} P_1/N_1 && \text{(5d)}
\end{aligned}$$

$$\begin{aligned}
dS_2/dt &= -\lambda_2^S S_2 + \eta^P P_2 + \mu(S_2^0 - S_2) + m_{12}\frac{S_1}{N_1} - m_{21}\frac{S_2}{N_2} && \text{(6a)}\\
dI_2/dt &= \lambda_2^S S_2 + \lambda_2^P P_2 - \alpha I_2 - \mu I_2 + m_{12}\frac{I_1}{N_1} - m_{21}\frac{I_2}{N_2} && \text{(6b)}\\
dR_2/dt &= \alpha I_2 - \eta^R R_2 - \mu R_2 + m_{12}\frac{R_1}{N_1} - m_{21}\frac{R_2}{N_2} && \text{(6c)}\\
dP_2/dt &= \eta^R R_2 - \eta^P P_2 - \lambda_2^P P_2 - \mu P_2 + m_{12}\frac{P_1}{N_1} - m_{21}\frac{P_2}{N_2} && \text{(6d)}
\end{aligned}$$

Now $\lambda_j^S = \beta^S r \frac{I_j}{N_j}$ and $\lambda_j^P = \beta^P r \frac{I_j}{N_j}$ for $j =$ cities $1, 2$ and $i = S, P$.

The populations of the two cities are constant if $m_{21} = m_{12}$. In this simple model with only one infection stage, we assume that infected people continue to travel with the same rate as the uninfected population. Thus the fraction of people traveling from city 2 to city

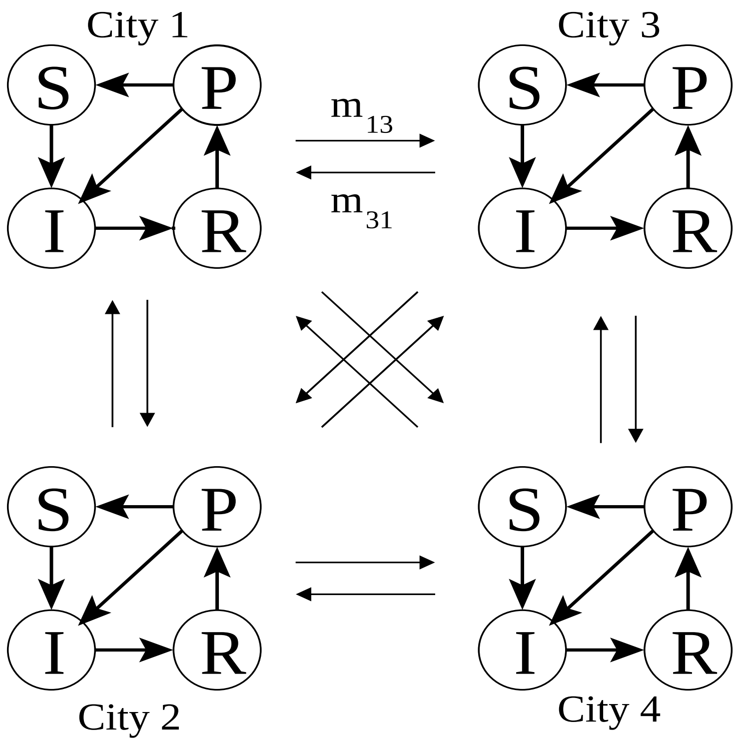

Figure 1: A schematic of how people travel through the stages of the illness and between the cities for a four city system. S-susceptible, I-infected, R-recovered(immune) P-partially susceptible. $m_{i,j}$-the number of people traveling from city i to city j per day.

1 that are infected is equal to the fraction of people in city 2 who are infected, (I_2/N_2). Consequently, the number of infected people entering city 2 from city 1 is $I_1\ m_{21}(I_2/N_2)$.

Figure 1 is a schematic of how people move through the stages of illness in a four city model. To generalize the two-city model to a multi-city model with n cities we first generalize the migration matrix M for the number of people traveling between cities;

$$M = \begin{pmatrix} m_{1,1} & m_{1,2} & \cdots & m_{1,n} \\ m_{2,1} & m_{2,2} & \cdots & m_{2,n} \\ \vdots & \vdots & \ddots & \vdots \\ m_{n,1} & m_{n,2} & \cdots & m_{n,n} \end{pmatrix}$$

Here m_{ij} is the number of people per unit time who travel from city i to city j. We have assumed that the simulation will be used for a short enough time that the migration matrix is constant. If the model is modified to allow the populations of the cities change, then the migration matrix must be recast as a function of the city populations. In our simulations M is symmetric, $m_{ij} = m_{ji}$, and therefore the population of each city remains constant. The diagonal terms, m_{ii}, account for all the non-travelers do not explicitly appear in the equations. The number of susceptible people entering city k is $\sum_{j=1}^{n} m_{jk}\frac{S_j}{N_j}$ and the number of susceptible people leaving city k is $\sum_{j=1}^{n} m_{kj} \frac{S_k}{N_k}$.

The resulting multi-city model is

$$dS_k/dt = -\lambda_k^S S_k + \eta^P P_k + \mu(S_{0k} - S_k) + \sum_{j=1}^{n} m_{jk} \frac{S_j}{N_j} - \sum_{j=1}^{n} m_{kj} \frac{S_k}{N_k} \quad (7a)$$

$$dI_k/dt = \lambda_k^S S_k + \lambda_k^P P_k - \alpha I_k - \mu I_k + \sum_{j=1}^{n} m_{jk} \frac{I_j}{N_j} - \sum_{j=1}^{n} m_{kj} \frac{I_k}{N_k} \quad (7b)$$

$$dR_k/dt = \alpha I_k - \eta^R R_k - \mu R_k + \sum_{j=1}^{n} m_{jk} \frac{R_j}{N_j} - \sum_{j=1}^{n} m_{kj} \frac{R_k}{N_k} \quad (7c)$$

$$dP_k/dt = \eta^R R_k - \eta^P P_k - \lambda_k^P P_k - \mu P_k + \sum_{j=1}^{n} m_{jk} \frac{P_j}{N_j} - \sum_{j=1}^{n} m_{kj} \frac{P_k}{N_k} \quad (7d)$$

Where rates of infection are $\lambda_k^S = \beta^S r \frac{I_k}{N_k}$ and $\lambda_k^P = \beta^P r \frac{I_k}{N_k}$ for each city $k = 1, \ldots, n$. This is a generalization of an earlier model studied by Hyman and Laforce [6].

3 Model Parameters

We establish model parameters appropriate for influenza virus in this section. Where possible, the parameters were obtained for strains of H3N2, the dominant strain of flu for the majority of our data set. The average illness lasts $1/\alpha$ days. We assume that rate of recovery from illness, α per day, is the same for all cities, regardless of location or season. We fix the duration of the infectious period to be 4.1 days, therefore $\alpha = 0.2439$. [1]

We assume that the infectiousness of an average infected person, the susceptibility of an average susceptible person, and the average number of contacts, is the same in all of the cities. All infected people are equally infectious and all fully susceptible people are equally likely to contract the illness. In a single person, infectivity is also assumed to be constant through the course of the illness. The infectiousness of an individual is higher in the winter than in the summer, regardless of the climate of the city. This may be do to increased infectiousness of the disease (β), or a change contact pattern of the average individual. This is reflected in the model by allowing the product $r\beta$ to be dependent on the season.

We define $\hat{\beta^S}$ as the mean infectivity per contact. Stilianakis et al. estimate the transmission rate as $\beta \approx 6 \times 10^{-4}$ in a randomly mixing population in the absence of drug resistance for a sub-clinical infection in [14]. We will use this as our baseline infectivity parameter. Sub-clinical infection is defined as an infection where a person is asymptomatic, but still infectious, and account for approximately 75% of all H3N2 infections [10].

Including a mechanism for previously infected people to return to susceptibility is a simple mechanism to account for the loss of immunity caused by the natural genetic drift of the virus away from the strain with which a person was infected, as opposed to an actual loss of immunity to a specific strain of the virus within a person. That is, we assume that the genetic strain of virus drifts at a constant rate, and that previously infected people slowly become susceptible to the currently circulating strain. The rates of return to partial and full susceptibility after illness are η^R and η^P. Frank et. al [4] reported no recorded cases of people becoming reinfected with H3N2 in the same season as a primary infection. Thus $\eta^R \leq 1/365 days$. That is, people are fully immune for at least a year.

Partially immune people are infected at a rate that is a fraction of the rate at which fully susceptible people are infected. Following full immunity, we allow a person to become partially susceptible to similar circulating strains of influenza. A person may have a partial immunity to the circulating strain of influenza for several years, or none at all, depending on the rate of drift of the virus. We define the time a person becomes partially immune when their susceptibility is the ratio $\sigma = (\beta^P/\beta^S)$ less than the susceptibility of people who have never been infected. In our simulations, we used a threshold of $\sigma = 0.55$ to define partially immune population. The average length of time a person is partially immune is unknown and we, arbitrarily, assign the period of partial immunity to be $\eta^P = 1/720 days$. We also assume that the length of time a person is infected is the same for both susceptible and partially immune people. In Section 5.1 we will show that the model is not sensitive to either of these parameters.

The model is insensitive to the rate μ at which people leave a city either by moving away or dying. We assigned the value $\mu = 0.0003 days^{-1}$, or that people live in a single city for approximately ten years before moving.

3.1 Estimation of $r\beta$ and ϵ

Two parameters must be estimated by fitting the available data. The number of adequate contacts a person has per day sufficient to transmit the disease, $r\beta$, and the amount which infectivity varies with the seasons, ϵ, are assumed to be the same for all of the cities. We fix $\beta = 6 \times 10^{-4}$ (the baseline value) and simultaneously estimate ϵ and r to fit the CDC data.

The CDC cities weekly mortality data set required some additional analysis before it could be used to estimate r and ϵ. We will also describe some of the variations and anomalies that had to be accounted for based on individual cities. To account for missing data in weeks where it was not reported, we estimated the number of cases for non-reporting weeks as the average value neighboring weeks that did report cases. For the purpose of fitting parameters, a weighting system w_i was used in which non-reporting weeks are assigned the value $w_i = 0$ and all other weeks are assigned the value $w_i = 1$.

Finally, the data is presented as weekly mortality while the model predicts daily morbidity. In order to make a comparison between the two, the mortality is assumed to be 1% of the morbidity and the number of deaths per week is divided up into an even number of cases every day. This assumption is a simple scaling parameter that can be accounted for by a simple multiplicative factor in the model predictions.

We define $model_t$ as the value predicted by the model at time t and $data_t$ is the CDC

meaning	parameter	baseline	suitable range
rate of recovery $(1/days)$ [1]	α	0.2439	$[0.07, 0.5]$
mean transmission probability per contact(fully susceptible) $(1/contacts)$[14]	$\hat{\beta^S}$	6×10^{-4}	$[5 \times 10^{-4}, 6 \times 10^{-3}]$
mean transmission probability per contact (partially susceptible) $(1/contacts)$	$\hat{\beta^P} = \sigma\hat{\beta^S}$	$\sigma = 0.55$	$[0.3, 0.7]$
seasonal fluctuation of transmission probability $(dimensionless)$	ϵ	0.0210	$[0.007, 0.026]$
number of contacts per unit time $(contacts/day)$	r	410.38	$[42, 625]$
number of adequate contacts per unit time $(contacts/day)$	$r\beta$	0.246	$[0.24, 0.26]$
removal rate of people from population in the absence of infection$(1/days)$	μ	0.0002740	$[0.000027, 0.25]$
rate of return to partial susceptibility $(1/days)$ [4]	η^R	0.00274	$[0.00137, 0.00274]$
rate of return to full susceptibility$(1/days)$	η^P	0.00137	$[0, 0.00549]$

Table 1: Model parameters, dimensions, baseline values used in the simulations, and estimated ranges of validity. Most of these parameters are assigned values estimated from the epidemiology literature. The two parameter, r and ϵ, whose values are unknown were determined by a least-squares fit so the model best matches the influenza data. The ranges for the average number of adequate contacts per day to transmit the disease, $r\beta$, and ϵ were chosen to reflect the differences between in the least-squares fit for different cities. The range for r was determined by dividing $r\beta$ by β.

data as defined in the last section. The residual

$$error = \sum_{t=1}^{n} w_t |data_t - model_t| \tag{8}$$

was then minimized in the l_1 norm using an alternating line search over ϵ and r until r converged to five significant figures of accuracy and ϵ converged to within three significant figures of accuracy. The l_1 norm is chosen because it minimizes the effect of outliers as compared with the l_2 norm.

To reduce the effect of outliers, we fit the data after smoothing it with a Hamming filter, $d_i \leftarrow (d_{i-1} + 2d_i + d_{i+1})/4$, three times. We observed that the minimizing values for ϵ and r, shown in Table 2, were not sensitive to the filtering process. We believe that the insensitivity to prefiltering the data may be because of the smoothing properties already inherent in the l_1 norm minimization procedures.

Because of uncertainties in the data, we chose to minimize the number of free parameters in the model and elected to find one value for ϵ and r for the entire data set. In order to choose these average values the cities Denver, San Francisco, Portland, Kansas City and Cincinnati were used because they had the smallest residuals. The model was then fitted over these five cities simultaneously to establish $r = 410.38$ and $\epsilon = 0.0210$ values for the entire data set.

Because in the model r always appears as a product with β, fitting r to data is equivalent to fitting the baseline value for the average number of adequate contacts per day to transmit the disease, $r\beta$. Therefore in the process of fitting the model to r, we also were correcting for uncertainty in β. The best fit for r is based on dividing the best fit for $r\beta$ by the baseline value for $\beta = 6 \times 10^{-4}$ [14]. This gives the baseline value $r = 410.38$, which seems to be high. If $\beta = 6 \times 10^{-3}$, then $r = 41.038$ average contacts per day.

The reproductive number is linearly related to the product $r\beta$. Thus this fit indirectly establishes a reproductive number consistent with the data. The model is more sensitive to the transmission rate $r\beta$, than to ϵ. Figure 2 illustrates the sensitivity of the least squares fit for r and ϵ. This will be discussed more in Section 5.1.

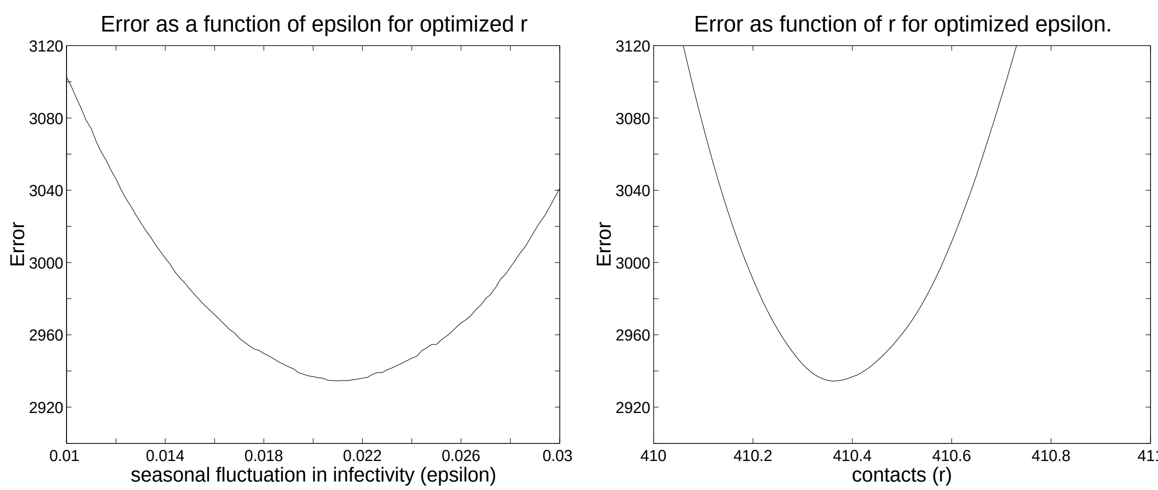

Figure 2: The residual in the l_1 norm over five cities for $\epsilon = [0.01, 0.03]$ with $r = 410.38$ and $\beta = 6 \times 10^{-4}$. The residual for $r = [410, 411]$ is plotted for with $\epsilon = 0.0210$ and $\beta = 6 \times 10^{-4}$. Note that if $\beta = 6 \times 10^{-3}$, then the best fit range for the number of contacts per day would be $r = [41.0, 41.1]$.

3.2 Population and Mobility

The population of each of the cities in Table 2 is based on the Census 2000 data [16]. In some instances, we combined the two major cities to account for the population in the area covered by the reporting station. There is some inconsistency in our population estimates because the population reporting to a CDC reporting station in a major city may be smaller than the population that uses the airport in the same city.

min over		entire	time
City	Population	r	ϵ
New York, NY	9314235	411.05	0.0154
Los Angeles, CA	9519338	409.89	0.0189
Chicago, IL	8272768	410.49	0.0093
Philadelphia, PA	5100931	410.49	0.0106
Washington, DC**	4923153	N/A	N/A
Detroit, MI**	4441551	N/A	N/A
Houston, TX	4177646	412.230	0.0119
San Francisco–Oakland, CA	4123740	410.12	0.0185
Atlanta, GA**	4112198	N/A	N/A
Dallas, TX	3519176	410.49	0.0200
Boston, MA	3406829	410.52	0.0216
Phoenix–Mesa, AZ	3251876	409.98	0.0236
Minneapolis–St Paul, MN	2968806	412.21	0.0240
Cleveland–Akron, OH	2945831	409.89	0.0251
San Diego, CA	2813833	411.57	0.0126
St. Louis, MO**	2603607	N/A	N/A
Baltimore, MD	2552994	412.17	0.0203
Seattle–Tacoma, WA	2414616	410.49	0.0129
Tampa–St. Petersburg, FL	2395997	412.76	0.0168
Pittsburgh, PA**	2358695	N/A	N/A
Miami, FL	2253362	410.49	0.0092
Denver	2109282	410.84	0.0207
Portland–Vancouver, OR	1918009	410.44	0.0269
Kansas City, MO–KS	1776062	409.89	0.0202
Cincinnati, OH–KY–IN	1646395	411.79	0.0147
Orlando*, FL	1644561	N/A	N/A
Sacramento, CA	1628197	415.89	0.0180
Fort Lauderdale*, FL	1623018	N/A	N/A
Indianapolis, IN	1607486	412.39	0.0069
San Antonio, TX	1592383	413.53	0.0249
Las Vegas, NV– AZ	1563282	412.60	0.0257
Columbus, OH	1540157	413.89	0.0179
Milwaukee–Waukesha, WI	1500741	411.64	0.0173
Totals:	107620755	411.1965	0.01368

Table 2: Populations of 33 largest cities in the US based on the 2000 census data and optimal r and ϵ fit for each city. *This city does not participate in the 122 Cities Mortality Reporting **This city's data was too noisy to obtain a parameter fit. [16]

Migration between cities is approximated by airline flight data for the third quarter of 2000 as posted on the US Department of Transportation web-site [11] in the Air Travel Consumer Report. The estimates are for the average number of one-way passenger trips per day between two cities. Thus for a city with more than one airport, such as New York, the flight statistics are for all of the airports combined. Some of the airline data is in Table 3.

Since the flight data is the total flights per day, half the flights are assumed to be going in each direction in the migration matrix in the model. This leads to a symmetric migration matrix where the same number of people enter and leave the city each day and a constant population for each city.

4 The 1996-2001 Influenza Seasons

The model assumption that there is only one strain of influenza circulating in the population is justified for the 1996-1997 influenza season through the 1999-2000 season, when the influenza A subtype H3N2 dominated. However the 1995-1996 and the 2000-2001 seasons were not decisively dominated by any one strain. In the 1997-2000 influenza seasons the epidemic threshold was exceeded for at least six weeks [2]. [17] [19] [18] In the 2000-2001 season the epidemic threshold was never reached, although this may be because the epidemic threshold was adjusted upward before this season [20]. The CDC data is summarized in Table 4.

The 122 Cities Mortality Reporting System is a volunteer system run by the participating cities. The cities each use their own system to count the P/I deaths and report the data directly to the CDC. There are inconsistencies in the data set due to changes in the volunteer staff and because there are often insufficient people to keep up with reporting during the peak of the influenza season [5]. The data also shows that some cities are more thorough in reporting than others. Also, there is uncertainty in the undercounting and what portion of P/I deaths may be attributed to influenza [5]. For the purposes of the model we assume that all influenza deaths are recorded and that all P/I deaths are attributable to influenza.

The data contains weeks in which no cases were reported. Frequently the unreported cases in one week are accounted for cumulatively in a single later report. Also, there is a lag time between the actual death dates and the report sent to the CDC. This lag time can be several weeks and tends to be longer in the winter than in the summer [5]. The CDC reports indicate that the office visits for influenza and P/I deaths peak with the mortality between 1 and 4 weeks after the morbidity peaks. The mean time between the morbidity peak and the mortality peak is 3 weeks. The reporting delay accounts for some of the time lag between the recorded peak of the epidemic as estimated through the physicians surveillance network and the peak of the CDC 122 cities influenza mortality epidemic. [2] [17] [19] [18] [20] We did not account for the time lag in our simulations and assumed that it was the same for all the reporting cities. If the reporting accuracy is estimated, then this could be used to adjust the data before defining the parameters. For example, to account for an estimated three-week time lag, a first order correction of the model is obtained by shifting the predictions back by the same time.

5 Model Threshold Conditions

The reproductive number, R_0, is the number of secondary infections that result from a single primary infection in a fully susceptible population. In a simple SIR model with no migration,

	New York, NY	Los Angeles, CA	Chicago, IL	Philadelphia, PA–NJ	Washington, DC	Detroit, MI	Houston, TX	San Francisco–Oakland, CA	Atlanta, GA	Dallas, TX	Boston, MA–NH	Phoenix–Mesa, AZ	Minneapolis–St. Paul,	Cleveland–Akron, OH	San Diego, CA	St. Louis, MO–IL	Baltimore, MD	Seattle, WA	Tampa–St. Petersburg, FL	Pittsburgh, PA	Miami, FL	Denver, CO	Portland–Vancouver, OR	Kansas City, MO–KS	Cincinnati, OH–KY–IN	Orlando, FL	Sacramento, CA	Fort Lauderdale, FL	Indianapolis, IN	San Antonio, TX	Las Vegas, NV–AZ	Columbus, OH	Milwaukee–Waukesha, WI
New York, NY		7324	7637	0*	5765	2953	2302	6055	6885	3382	6566	1318	2103	1136	1338	1117	398	1590	3485	1377	3342	2560	737	939	994	7658	302	7675	849	411	4414	856	826
Los Angeles, CA			3986	1289	1929	1559	1363	8220	1611	1576	1993	3162	1323	647	311	747	1582	2997	542	424	816	2075	1662	735	395	1258	2229	527	826	419	5324	462	522
Chicago, IL				2313	2783	3673	1943	3468	3711	3140	2579	2265	4049	2591	1144	2735	2933	1649	1836	965	918	2820	786	2555	762	2657	475	1566	867	542	3084	1291	0*
Philadelphia, PA–NJ					0*	848	719	1268	2553	1054	1561	548	634	322	505	402	0*	529	1040	750	461	629	175	319	358	1882	0*	1058	370	0*	1332	278	323
Washington, DC						618	881	1426	3221	1919	3307	321	1242	304	610	420	0*	749	990	319	1016	1415	248	584	414	1807	185	887	318	361	381	443	456
Detroit, MI							693	927	1699	992	661	853	1095	127	450	1196	951	675	946	219	369	616	291	534	225	1550	0*	562	517	189	1700	0*	466
Houston, TX								1081	1645	5652	751	598	448	479	465	793	863	606	440	255	418	930	274	533	195	790	191	365	341	944	1053	269	0*
San Francisco–Oakland, CA									1313	1530	1951	2427	1577	505	5041	451	1570	4615	326	471	543	2320	2653	551	378	643	0*	264	395	174	4310	341	614
Atlanta, GA										2855	2552	618	1307	596	560	653	1320	785	1914	765	1564	1249	420	856	493	2060	262	1774	437	391	865	496	396
Dallas, TX											1327	939	1244	382	710	821	529	939	768	354	470	1989	473	1187	314	1143	257	588	407	2228	1429	378	397
Boston, MA–NH												422	1312	445	574	317	759	695	1006	648	540	1358	282	371	425	1627	132	1332	321	0*	822	450	389
Phoenix–Mesa, AZ													1186	458	2351	568	928	1444	235	233	133	1353	1027	564	206	414	797	217	492	291	2578	448	377
Minneapolis–St. Paul,														346	625	539	311	1353	321	375	242	1770	429	860	405	986	226	181	291	316	1123	227	773
Cleveland–Akron, OH															260	639	1449	282	410	0*	179	342	0*	293	0*	651	0*	340	182	0*	714	0*	220
San Diego, CA																363	899	1614	204	192	0*	1103	929	371	0*	324	2023	202	244	182	2136	230	161
St. Louis, MO–IL																	1170	501	496	157	131	481	242	1033	176	716	0*	310	339	298	489	459	0*
Baltimore, MD																		796	1127	0*	313	818	463	537	177	1436	324	911	502	445	1093	32	0*
Seattle, WA																			291	266	172	1438	554	431	245	535	1258	238	294	230	2021	323	341
Tampa–St. Petersburg, FL																				457	328	459	0*	348	284	0*	0*	1244	582	0*	646	664	204
Pittsburgh, PA																					150	390	0*	211	0*	582	0*	309	0*	0*	348	0*	0*
Miami, FL																						328	0*	156	172	308	0*	0*	109	0*	512	118	101
Denver, CO																							870	1249	435	766	401	205	351	263	1248	246	385
Portland–Vancouver, OR																								262	0*	298	1197	0*	0*	0*	1296	173	0*
Kansas City, MO–KS																									195	699	228	156	322	204	729	219	216
Cincinnati, OH–KY–IN																										376	0*	216	0*	0*	246	0	0*
Orlando, FL																											190	798	975	264	660	818	623
Sacramento, CA																												0*	0*	0*	1143	0*	0*
Fort Lauderdale, FL																													337	0*	561	281	124
Indianapolis, IN																														0*	860	0*	0*
San Antonio, TX																															588	0*	0*
Las Vegas, NV– AZ																																937	792
Columbus, OH																																	0*
Milwaukee–Waukesha, WI																																	

Table 3: Daily flights between 33 major US cities[11] * Market not large enough to be listed in top 1000 U.S markets.

Influenza Season	Week influenza morbidity peaked	Week influenza mortality peaked	Predominant strain	Percent which are predominant strain	Number of weeks epidemic threshold exceeded
1995-1996	Jan 6-13	Jan 20	A(H1N1)	50	6
1996-1997	Dec 28	Jan 25	A(H3N2)	78	10
1997-1998	Feb 7	Feb 28*	A(H3N2)	99.5	11
1998-1999	Feb 6-27	March 13	A(H3N2)	76	12
1999-2000	Jan 1	Jan 22	A(H3N2)	96.5	22
2000-2001	Feb 3-10	Feb 24*	A(H1N1)	52	0

Table 4: Summary of the data reported by the CDC in their Surveillance for Influenza reports for 1995–1996 through 2000-2001 influenza seasons. Note that the influenza mortality peaks about three weeks after influenza activity, [2] [17] [19] [18] [20]. *The week in which influenza mortality peaked was not provided in the report, so the week in which influenza activity peaked + three weeks is used.

time dependence on transmission probability or return to susceptibility, as outlined in Section 2.1 $R_0 = r\beta/\alpha$. If $R_0 > 1$, then the epidemic spreads within the population to a stable equilibrium value. If $R_0 < 1$, then the only stable equilibrium is the zero equilibrium and the epidemic dies out.

For more complex models, the reproductive number is determined by the dominant eigenvalue of the Jacobian matrix at the infection free equilibrium [7]. The reproductive number for the network of n cities can be found by solving the eigenvalues of the $4n \times 4n$ Jacobian matrix for the multicity model (7). As the parameters change, the eigenvalues must be recalculated for each case.

Often a simple analytic formula for the threshold conditions (T_0) estimating when the epidemic will take off and when it will die out can give more insight into the behavior of an epidemic than computing the reproductive number for a specific set of parameters. We found it useful to analytically calculate the reproductive number for each city assuming that it is isolated and then to use this as a guide to estimate a threshold reproductive number for the entire population.

An upper bound for R_{0k} for the k-th city is limited by the maximum of the time dependent infectivity, $\beta = \beta_{max}$. That is $R_0 = \max[r\beta_k/(\phi_k + \alpha)]$. Here $1/(\phi_k + \alpha)$ is the average time a person is infected and remains in the k-th city. To account for the natural removal rate, μ, and the migration of people from the population in a city addition to the fraction of people who leave city k for other cities per unit time, we define $\phi_k = \mu + \sum_{i=1}^{n} D_{k,i}$.

We define an upper bound for threshold condition for the multicity system by defining it to be the maximum reproductive number of any of the cities, because if the epidemic spreads in one city then it will persist in the entire population. That is,

$$T_0 = \max(R_{0k}) \text{ for k = 1, \ldots ,n}$$

While only a threshold value, not a reproductive number, T_0 provides an accurate indication if an epidemic in a multi-city population will persist or die out. For the baseline parameters in Table 1, the $T_0 = 1.02$ and occurs in Pittsburgh. Because $R_0 \approx T_0 \approx 1$, the model is sensitive to small changes in βr. If $\epsilon > 0.02$, then effective reproductive number of the system falls below one in the summer seasons, indicating that influenza cannot persist long under summer conditions. We were surprised at how closely our model and estimated parameters resulted in predicting that the annual influenza epidemic is perched precariously close to being able to sustain itself.

Because T_0 and R_0 depend linearly on the number of contacts per day, this implies that one of the most effective strategies to slowing the initial outbreak of an epidemic with $R_0 \approx 1$, like influenza or SARS, would be for people to limit the number of adequate contacts with other individuals during the epidemic. When this approach is applied in the early stages of and epidemic, as the World Health Organization did for SARS in Toronto [3], then there is a good chance to contain the early spread of epidemic. The dependence on the connectivity ϕ to other cities on threshold conditions is less obvious.

5.1 Sensitivity Analysis

The relative sensitivity of the model prediction to small changes in each parameter can help determine the most important parameters in slowing the epidemic. The normalized sensitivity of five quantities (I_{max}, I_{min}, $I_{cumulative}$, S_{max}, and S_{min}) with respect to each of the eight parameters is approximated by

$$\frac{dQ}{dp}\frac{1}{Q_0} \approx \frac{[Q_{p(1+\delta)} - Q_{p(1-\delta)}]/Q_0}{[p(1+\delta) - p(1-\delta)]/p_0} \tag{9}$$

where δ is the percent change in each of the parameters, Q = (I_{max}, I_{min}, $I_{cumulative}$, S_{max}, and S_{min} and p = r, β^S, β^P, α, μ, η^R, η^P, and ϵ. The factor $1/Q_0$ normalizes the importance of each parameter with respect to Q so the relative importance of the parameters can be compared.

The parameter α, the rate of recovery from infection, is the most important single parameter in every quantity we evaluated. For the baseline case, a 1% change in α results in a 122% change in peak of the infected population and a 1.5% change in the susceptible population.

The model is also sensitive to changes in β^S and r, the mean infection rate per contact for fully susceptible people and the number of contacts per unit time, respectively. The two quantities always appear in a product and have approximately equal importance in the model. A 1% change in either parameter yields approximately a 120% change in the peak of infected population and a 1.5% change in the susceptible population.

The infection terms I_{max}, I_{min} and $I_{cumulative}$ are three orders of magnitude less sensitive to β_P, η^R and η^P than they were to β^S and r. A 1% change in β_P, η^R or η^P results a [0.53%–0.35%] change in the infected population. A 1% change in these parameters yields only a 0.002% change in the susceptible population.

The epidemic is also relatively insensitive to ϵ. A 1% change in ϵ results in a 0.3% change in I_{max} and I_{min}. None of the other measurements are significantly affected by this parameter.

For simulations of a couple of years, the predictions are insensitive to changes in the migration/natural death rate, μ. These terms have such a small impact that they could be eliminated without significantly effecting the results.

In the model, the peak of the epidemic does not occur at the same time as the peak in the infectivity. The time lag follows from the seasonal variation in the infectivity and can be estimated from an approximate solution for the infected stage in a single city model. When the multi-city model is in periodic equilibrium the same fraction of people are infected in each city. Therefore, the same number of infected people are entering a city as leaving, and the migration terms balance. When the multicity model is at equilibrium, the reduced equation for the infected stage in a city is

$$\frac{dI}{dt} = \lambda^S S + \lambda^P P - \alpha I - \mu I \tag{10}$$

or, in terms of the basic parameters,

$$\frac{dI}{dt} = I(\hat{\beta^S}\hat{r}(\frac{S}{N} + \sigma\frac{P}{N})(1 + \epsilon sin(\tau t)) - (\alpha + \mu)) \tag{11}$$

To simplify notation, we define

$$\begin{aligned} a(t) &= \hat{\beta^S}\hat{r}(\frac{S(t)}{N} + \sigma\frac{P(t)}{N}) && \text{(12a)} \\ b &= -(\alpha + \mu) && \text{(12b)} \end{aligned}$$

and rewrite the equation as

$$\frac{dI}{dt} = I(a(t)(1 + \epsilon sin(\tau t) + b) \tag{13}$$

After some time $\hat{t}$, the model with the baseline parameters settles down into a solution with period τ. In this periodic solution, the difference between the maxima and the minima of the number of people in the susceptible and partially susceptible populations changes by approximately one percent and $\hat{t}$ $a(t) \approx a$ is constant. The simplified equation

$$\frac{dI}{dt} = I(a(1 + \epsilon sin(\tau t) + b) \tag{14}$$

and solution

$$I = Ce^{(a+b)t}e^{-\frac{a\epsilon}{\tau}cos(\tau t)} \tag{15}$$

accounts for the $\tau/4$ lag in the peak of the infection every year provided that $e^{(a+b)t}$ is bounded.

For the baseline parameters, we verified that $a(t) \in [0.2445, 0.2447]$ for $t > \hat{t}$ days. Therefore $(a+b) \in [-7.66 \times 10^{-5}, 7.25 \times 10^{-5}]$, and

$$I \approx Ce^{-\frac{a\epsilon}{\tau} cos(\tau t)} \tag{16}$$

which is periodic with period τ. This provides an accurate estimate for time lag between the peak of the infectivity and the peak of the epidemic. This time lag might be an important factor that should be considered when studying the theory on the influence of the cold weather on the survival of the virus. That is, changes in people behavior during the winter months may give the virus a window of rapid transmission, the effects of which are not felt until much later.

6 Numerical Simulations

The model equations were integrated numerically with a variable order Adams-Bashforth-Moulton Matlab solver, ode113. The parameters were set to the baseline values in Table 1 with the network of the 33 cities listed in Table 3, unless otherwise noted.

The influenza subtype H3N2 first became a dominate strain in the pandemic of 1968 [15]. We assumed that recent infections for this strain is close to a periodic equilibrium and used it as the benchmark data to be compared with the simulated model periodic equilibrium.

A small initial infection was introduced into the model and the solution was integrated until it reached periodic equilibrium. The timing for the model was set by the time that the largest fraction of people in each city is infected. In the periodic equilibrium, the same percent of people are in each stage in each city. At the peak of the epidemic, we observed 98.76% of people susceptible, 0.005731% of people infected, 0.4503% of people recovered and 0.7854% of people partially immune. The solution of the model, shown if Figures 3, 4, 5,6 and 7, illustrate that some of the cities report data close to the model predictions, while others differ greatly. The smooth curves in the figures are the model predictions, while CDC P/I data plotted is highly variable.

The magnitude of the epidemic in Los Angeles, and Kansas City is slightly over estimated by the model, however the prediction is quite good. The data for New York City is fit quite nicely by the data, although the number of cases is slightly underestimated by the model. The over estimates occur in the first two seasons, then for the last two influenza seasons the model fit is reasonable. The data for San Francisco/Oakland, Boston, Phoenix, Denver and Portland are well predicted by the model. In all five cities the seasonal variation in the number of cases is greater than that predicted by the model.

Neither Chicago nor Philadelphia were cities used to fit the parameters in the model. Even so, they were two of the cities where the magnitude and seasonal fluctuation of the yearly epidemic was well approximated by the model.

Indianapolis, Milwaukee, and Cincinnati are all slightly underestimated by the model. Note that Indianapolis and Milwaukee seem to have very little seasonal variation in the number of P/I deaths, unlike most of the other cities posting consistent data, this is surprising as the cold weather in these cities would be expected to increase the seasonal variation in the epidemic.

The influenza mortality for Minneapolis, San Diego and Las Vegas is underestimated by the model. This is likely because of differing (or more comprehensive) data collection techniques employed in these cities.

The model prediction of the mortality for Houston, Baltimore, Tampa, Sacramento, San Antonio and Columbus is substantially lower than the actual data. There are a number of potential reasons for this. One is that the population base used for the data collection is of the metro area, as opposed to the city proper, as was assumed in the model. Another is that these cities collect more complete data than the other cities or that they have a more liberal criteria for classifying cause of death as P/I. We did not identify any correlation between the reported data and the climate in these cities. However, it could be significant that four of these cities are among the six smallest in the model. This might indicate that even in populations as large as the these cities, the size of the population might still affect the number of contacts. Recall that the model predictions are sensitive to the number of contacts per day for a typical individual.

The CDC mortality is inconsistent for Detroit, Dallas, Cleveland, Seattle and Miami. In the last two years these cities reported significantly more influenza deaths. Whether this is because of a new method of data collection, a larger population base being used, or a genuine change in the number of P/I deaths is unknown. As none of the other cities showed a substantial increase in reported P/I deaths in this time frame it seems likely that a change in data collection took place. What is significant is that in all five cases the higher estimates were similar with what the model predicted. It seems likely that the new data collection method was comparable with that of the cities which the model was fitted to, thus a good prediction was obtained.

The data for Washington, St. Louis, Atlanta (Not Shown) and Pittsburgh is substantially lower than predicted by the model. These four cities turned in very low estimates for the five years of the data set compared to the other cities we studied. This could be because they were using a small subset of the population to approximate the whole, or because they had a very stringent definition of what was recorded as a P/I death. Atlanta was included in the model as the ninth largest city in the U.S., however the fit is not shown because they stopped collecting data for most of 1999 and 2000.

The data does not support a correlation between climate and number of influenza deaths. It was anticipated that, since the infectivity and contact rate are constant for all of the cities, the model would underestimate the number of influenza cases in the cities with harsher climates. In fact two of the cities for which the model underestimates the number of deaths the most are Houston, TX and Sacramento, CA both of which have warm climates.

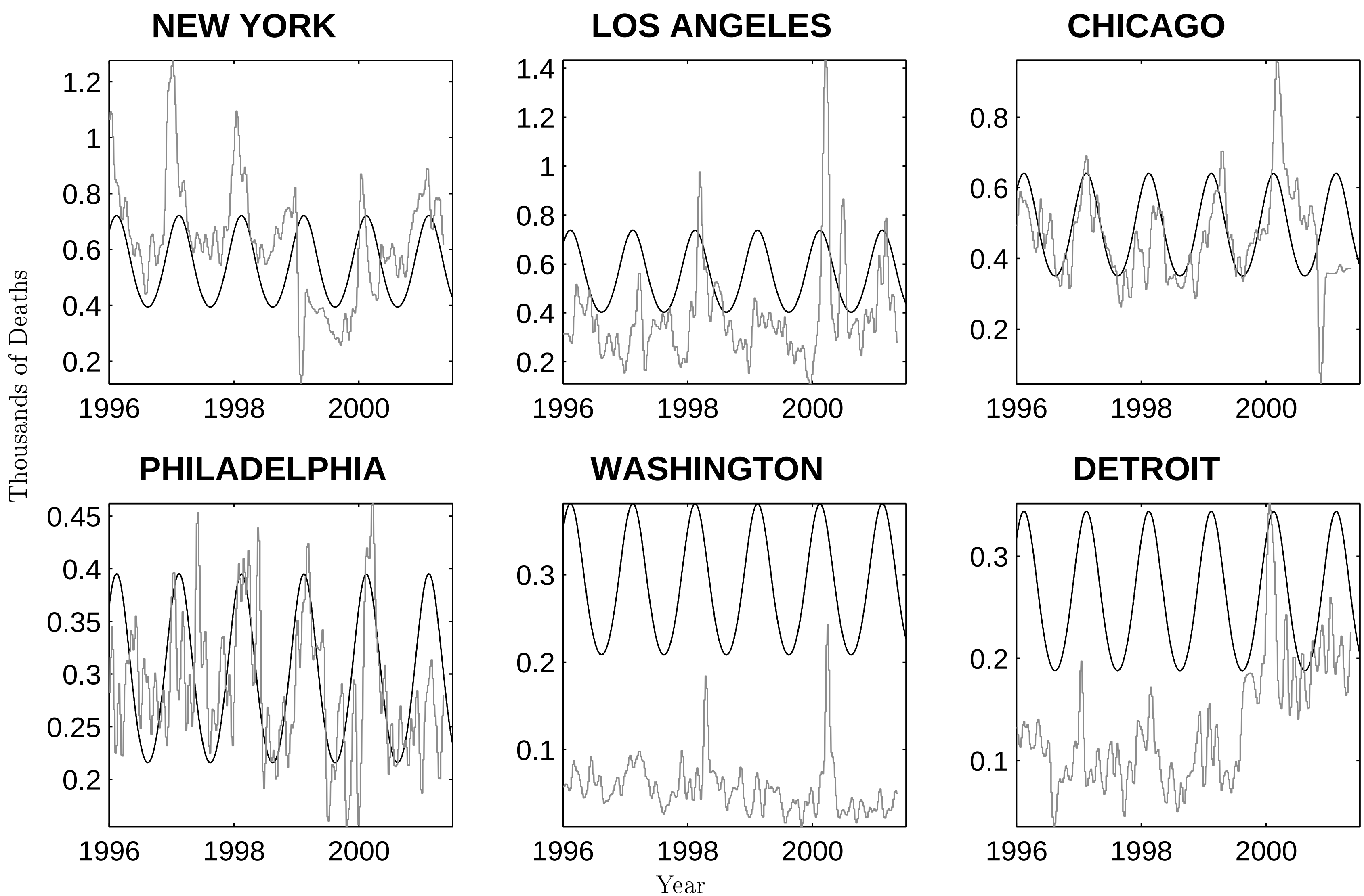

Figure 3: Comparison of the results of the simulation with data from the Centers for Disease Control [2] [17] [19] [18] [20]

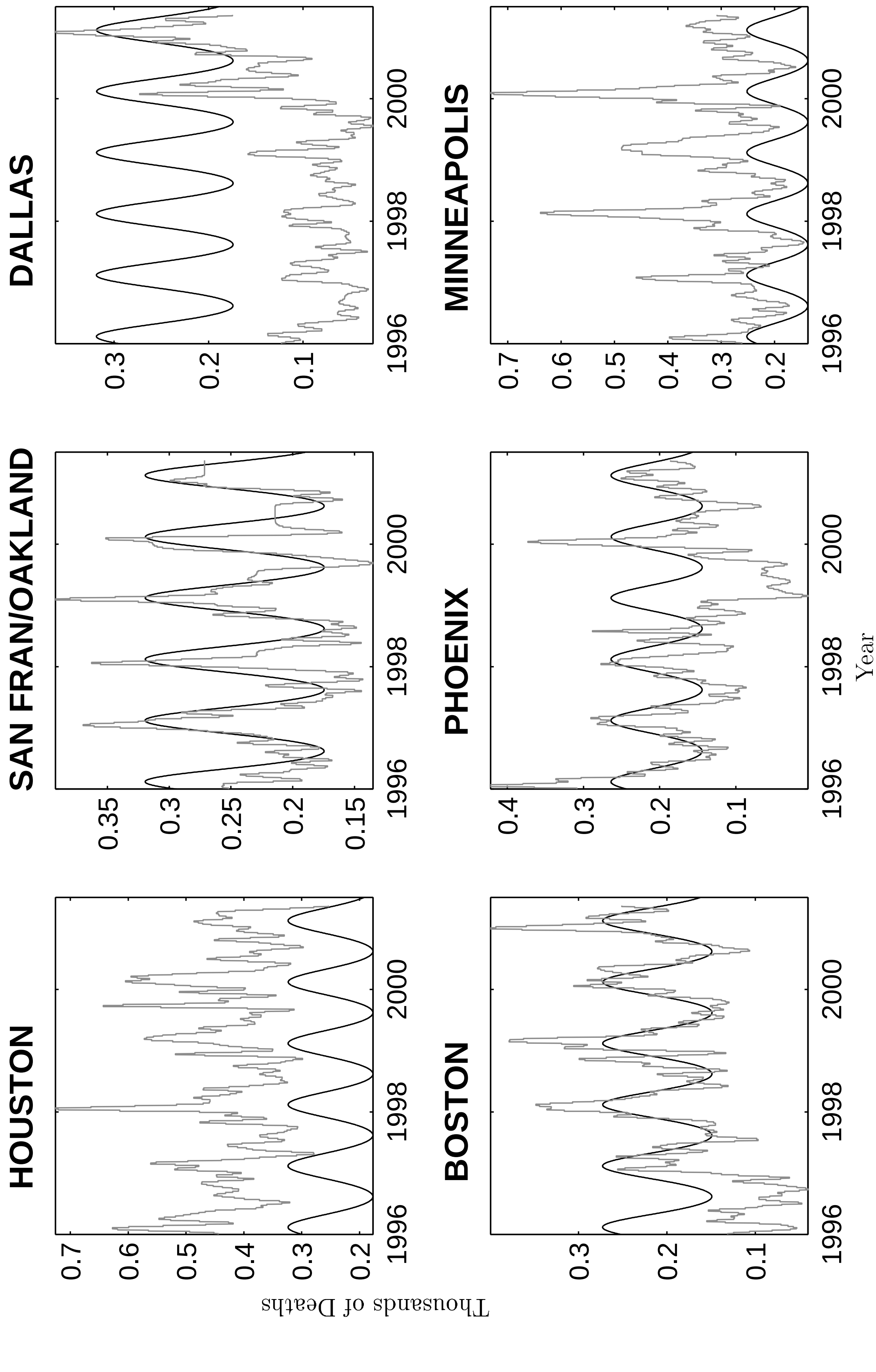

Figure 4: Comparison of the results of the simulation with data from the Centers for Disease Control [2] [17] [19] [18] [20]

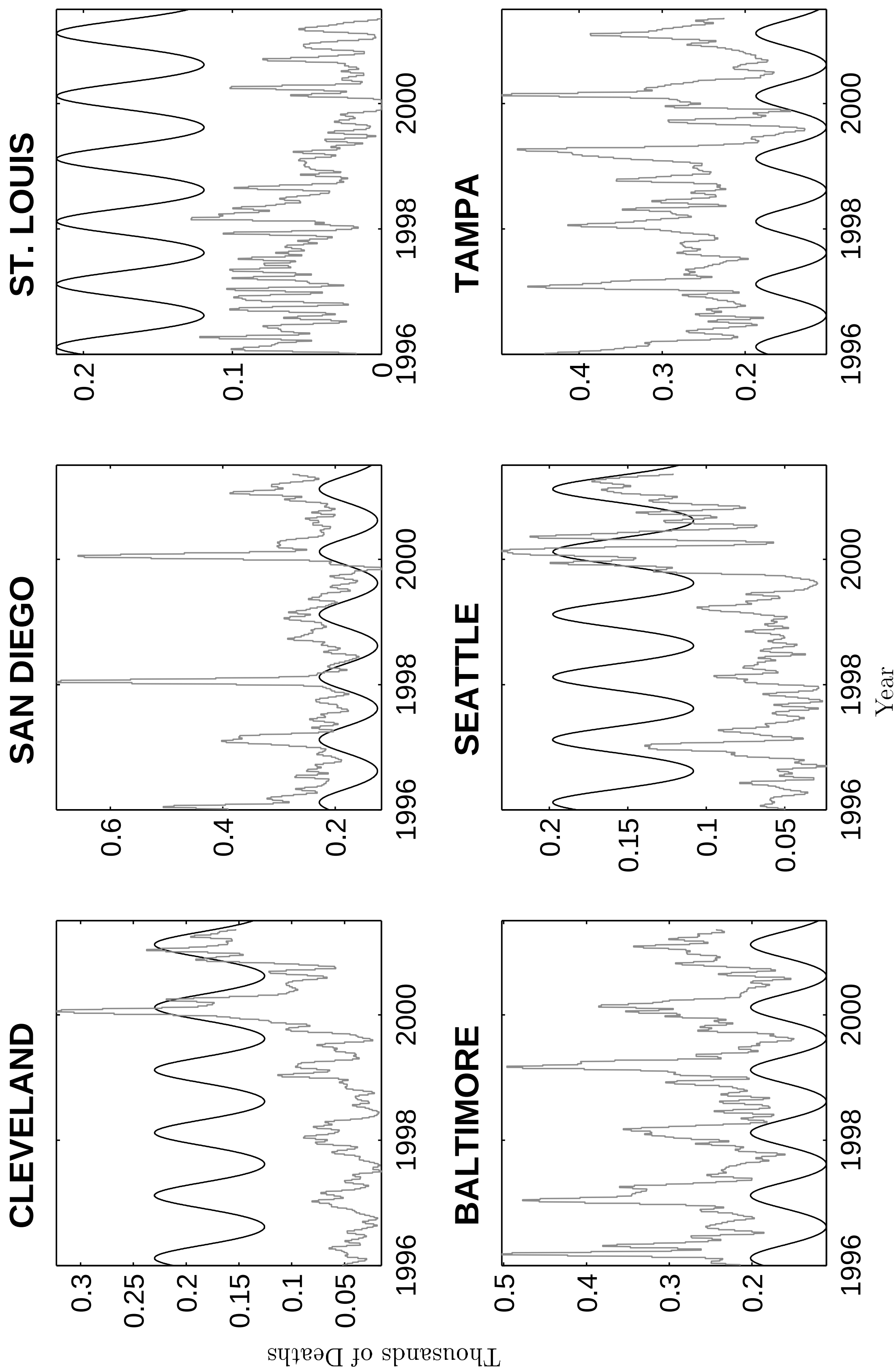

Figure 5: Comparison of the results of the simulation with data from the Centers for Disease Control [2] [17] [19] [18] [20]

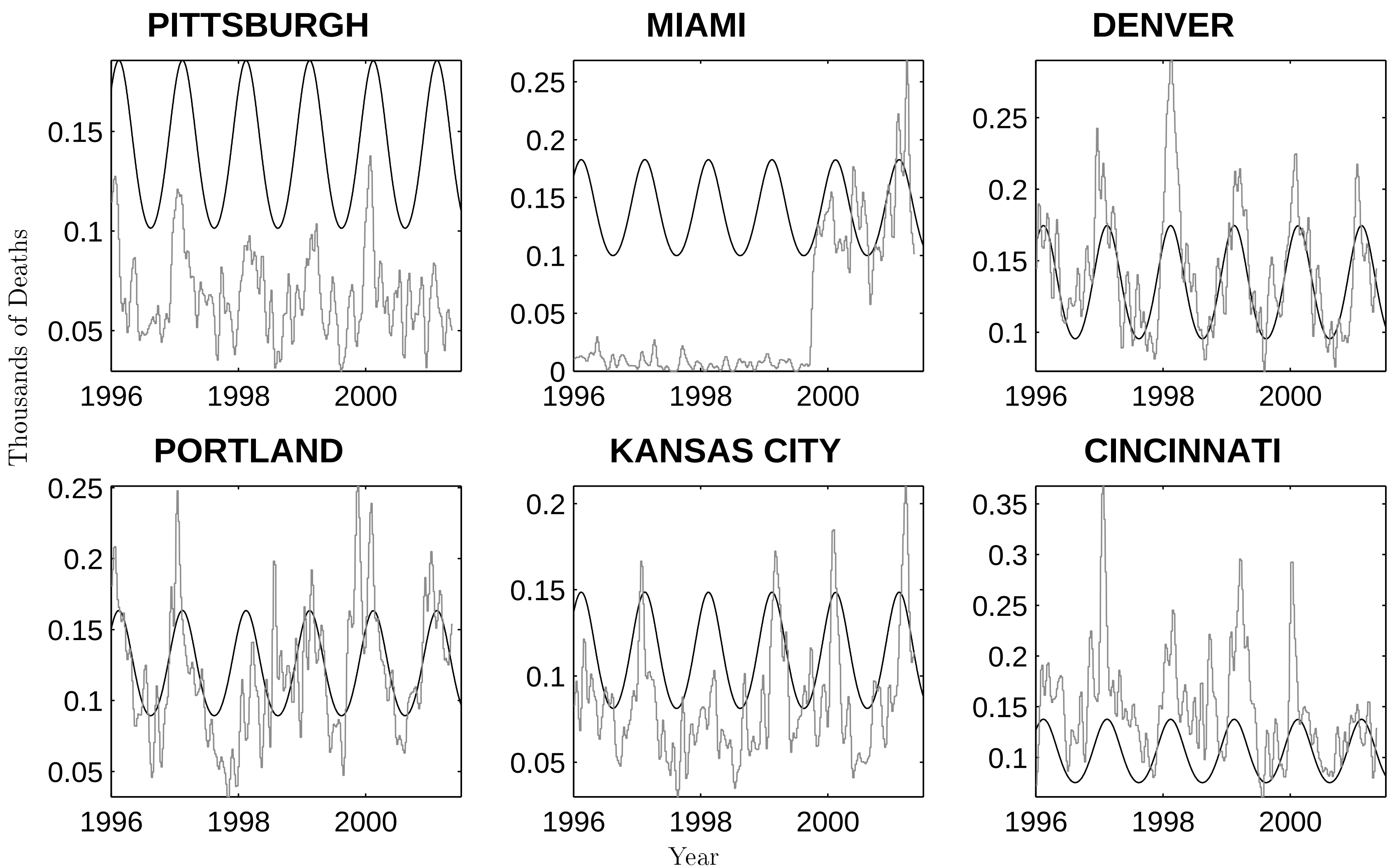

Figure 6: Comparison of the results of the simulation with data from the Centers for Disease Control [2] [17] [19] [18] [20]

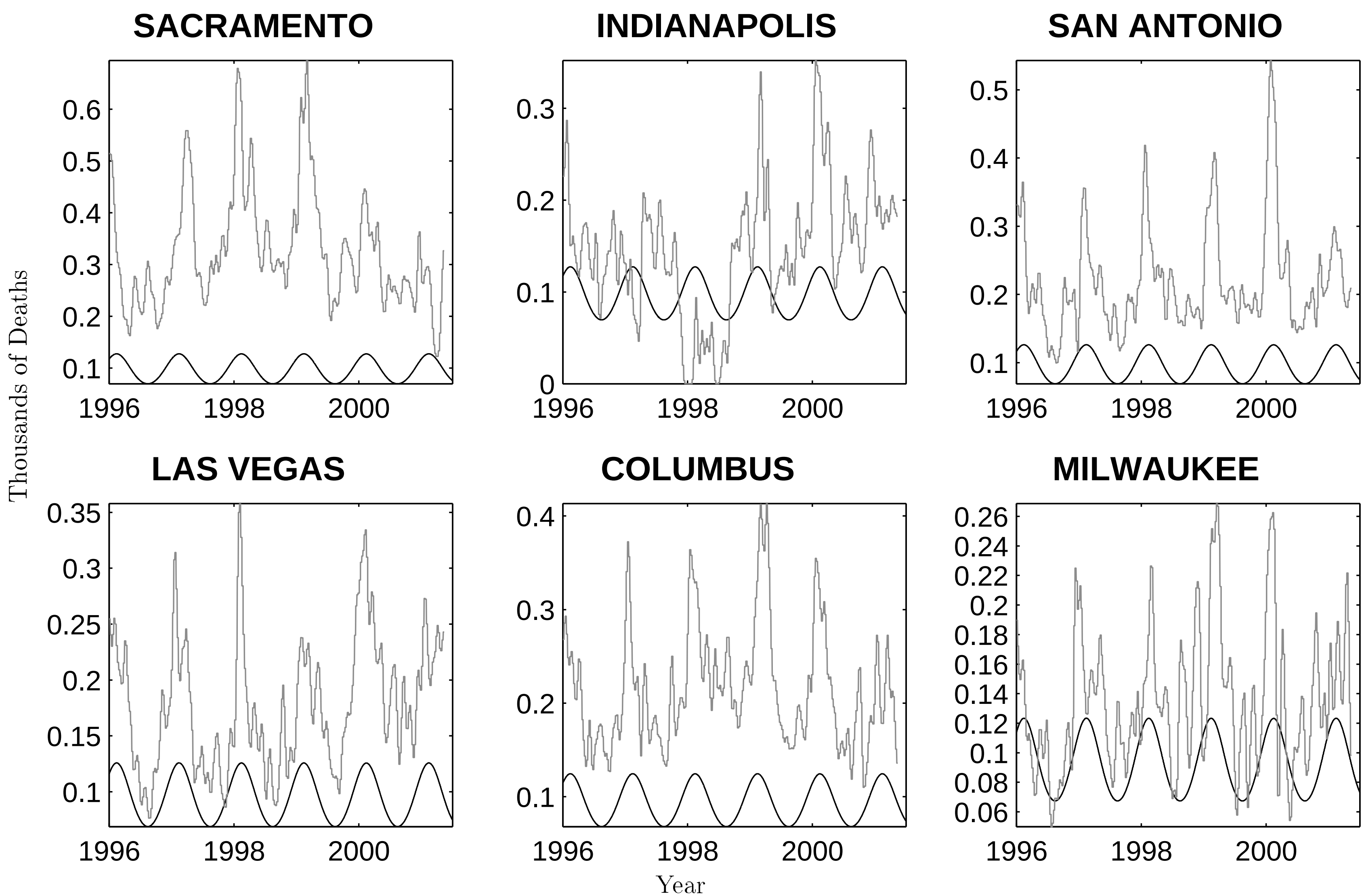

Figure 7: Comparison of the results of the simulation with data from the Centers for Disease Control [2] [17] [19] [18] [20]

6.1 Initial Stages of an Epidemic

In the initial outbreak the size of the network of cities has a substantial impact on the early spread of the epidemic. We formulated the model on a subset of the major cities of the United States. At the periodic equilibrium, running the reduced models yields the same results as the full model because the same percentage of people in each city are infected. Therefore the same number of infected people are leaving each city as entering. This is not true for the transient epidemic before it reaches the equilibrium. The recent SARS epidemic demonstrated how quickly an infection can spread from a local outbreak to a global problem. For these simulations the epidemic is assumed to start in a single city (New York) and spread outward from there.

In our simulation, the epidemic is started with 1000 people ill, as it would take a reasonably large number of people getting infected before an emerging epidemic is identified. We investigated how the size of the subset of cities in the network affects the spread of the epidemic. We observed that the smaller the network is, the faster the epidemic approaches equilibrium. Also, in smaller networks it spreads in the city of the initial outbreak because of the larger reproductive number resulting from fewer people migrating into and out of the city. The Figure 8 shows the initial outbreak for an epidemic that emerged on the day of highest infectivity (in November).

The severity of the initial epidemic is dependes on when the epidemic emerges. The Figure 9 shows the initial outbreak for an epidemic that emerged one three months earlier than the day of highest infectivity (in August).

7 Discussion

We defined a modified SIR model for the spread of influenza that accounts for non-random mixing among a discrete network of 33 cities. The nodes of the network were weighted by the population of the city and the bonds between the nodes represented the daily movement of people among the data as estimated by airline flight data. Data from the influenza transmission studies, and the reported mortality data attributed to influenza and pneumonia were used to define the model parameters. Despite noise in the 122 Cities data from the CDC, similar estimates for fluctuation in infectivity and number of contacts (and thus reproductive numbers) are obtained for each city.

The essential features of the yearly influenza epidemic approximated the influenza and pneumonia mortality data reported by Centers for Disease Control and Prevention. The magnitude and fluctuation of the yearly epidemic is well matched by the prediction of the model at the periodic equilibrium. At the endemic equilibrium the travel terms in this model are not important.

We observed that the threshold reproductive number for the network of cities is very close to one and that the model predictions are most sensitive to α and $r\beta$. That is, the most effective approaches to slowing an epidemic is to treat the ill to reduce the length of

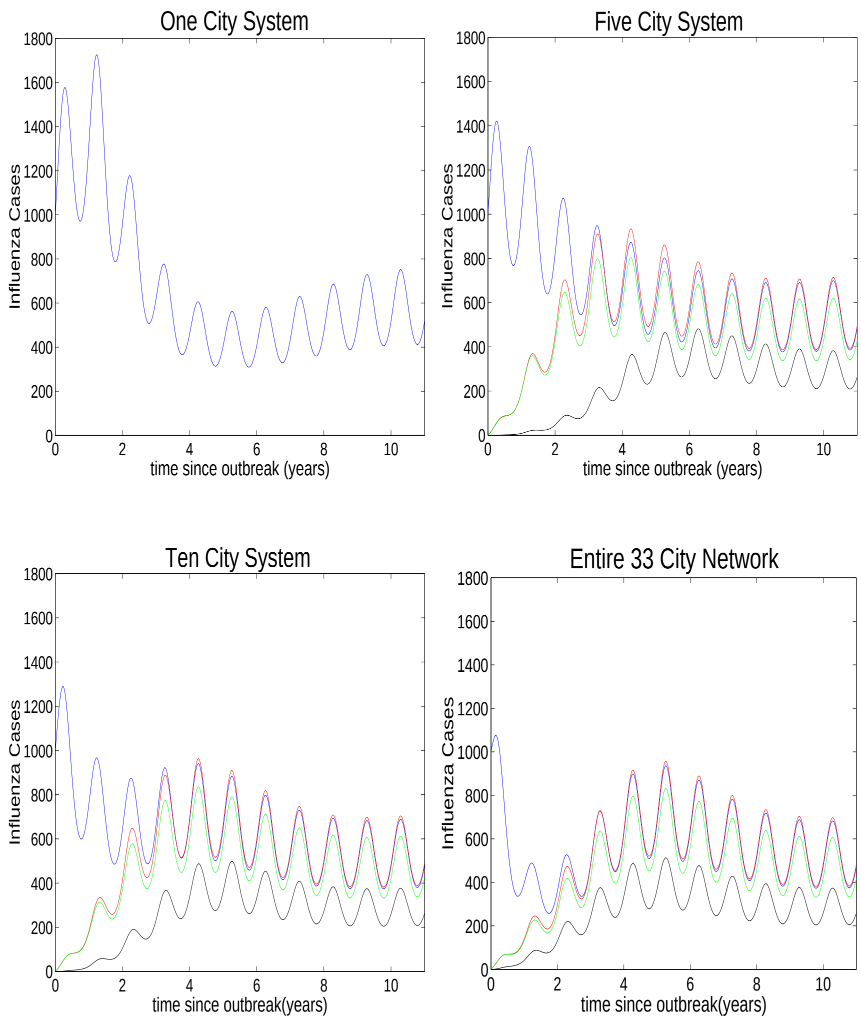

Figure 8: Initial outbreaks for various size systems of cities when the outbreaks starts at the time of peak infectivity. Subfigure 1 is for New York alone. Subfigure 2 is for the largest 4 cities in the US on a network of the largest 5 cities in the US. Subfigure 3 is the results of the largest 4 cities in the US on a network of the largest 10 cities in the US. Subfigure 4 is the results of the largest 4 cities in the US on the entire 33 city network.

the infectious stage (α), to reduce the number of contacts an infected has in a typical day (r), and to reduce the probably of transmission in a typical contact (β). These are precisely the measures taken in Toronto to contain the initial spread of SARS and were demonstrated to be highly effective [3].

There is a substantial time lag between the peak of the infectivity and the peak of the epidemic, which is accounted for by deriving an approximate solution to the differential equation of the infected stage.

We also used the model to predict the initial spread of a new infectious agent when it is introduced into one of the cities. In the initial stages of the epidemic, the number of cities in the network and the timing of the outbreak determine how the epidemic spreads within

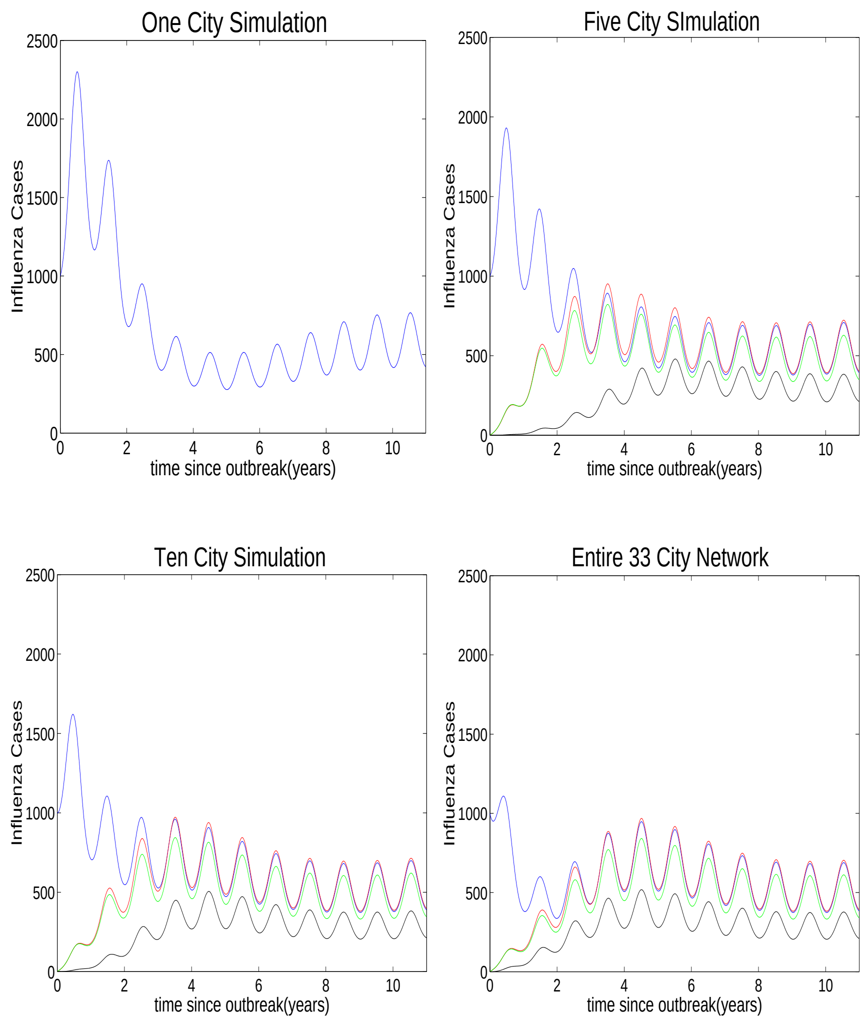

Figure 9: Initial outbreaks for various size systems of cities when the outbreak starts during the lower infectivity season. Subfigure 1 is for New York alone. Subfigure 2 is for the largest 4 cities in the US on a network of the largest 5 cities in the US. Subfigure 3 is the results of the largest 4 cities in the US on a nework of the largest 10 cities in the US. Subfigure 4 is the results of the largest 4 cities in the US on the entire 33 city network.

and among each of the cities.

One area of primary concern in the model is the assumption of random mixing of the populations within the cities. However, people within cities have groups, based or age, geographic, socio-economic, or religious affiliation, that they mix with regularly and have fairly few contacts with people outside of them. Additionally, a small portion of the citizens of a city will do the majority of the traveling. This suggests the development of a model which has non-randomly mixing groups called a small world model within each city in addition to the travel between cities. Some of the groups would travel more often than others. A first step in this direction would be to have a model with two groups in each city, travelers and non-travelers. We have observed in more detailed biased mixing models that after a brief startup period, the random mixing assumption is fairly accurate.

In the model the same fraction of people in each city are susceptible, infected, immune and partially susceptible to the epidemic at periodic equilibrium. This is a result of the contact rate and infectivity being the same for each city. This assumption has been used in other multi-city SIR models [12] with good results. However uniform contacts is not an appropriate assumption for the early stages of an epidemic because of the nonrandom mixing of the population, variations in the population density, and availability of public transportation in different cities. A better approach would be to fit contact rates to the data for subsets of cities based on availability of public transportation or population density.

The populations of the cities was kept constant by not including any increased mortality due to influenza. As long as we are concerned only with the endemic equilibrium and the annual influenza epidemic this assumption is reasonable. However for longer term simulations, or more severe epidemics, the increased mortality due to influenza must be accounted for.

The current model accounts for a slight drift in the genetic code for one strain of influenza by allowing a previously infected person to gradually lose immunity to the currently circulating strain of the virus. This is a reasonable assumption in a simulation of two or three years if the annual influenza epidemic is decisively dominated by a single strain. It will not predict the impact of a major shift in the virus. A straight forward extension of the model could account for multiple strains. However, there is very little data on the strain that causes a particular infection or the variation of the susceptibility of the population to different stains needed to validate the model.

Acknowledgements: We thank Lori Hutwagner, CDC Epidemiology Program for answering questions about the 122 Cities Mortality Data, Lynetter Brammer, CDC Influenza Branch for answering questions about the Physicians Surveillance Network and Leon Arriola for help analyzing the model. We also thank Bill Sailor, Shilpa Khatri, Thomas Park, Miriam Nuno, and Andy Perelson for their help and feedback on the paper and Mike McKay for his comments on the sensitivity analysis.

References

[1] C.L. Addy, I.M. Longini, and M. Haber. A generalized stochastic-model for the analysis of infectious-disease final size data. *Biometrics*, 47(3):961 – 974, 1991.

[2] T. Lynnette Brammer, Hector S. Izurieta, Keiji Fukuda, Leone M. Schmeltz, Helen L. Regnery, Henrietta E. Hall, and Nancy J. Cox. Surveillance for influenza — United States, 1994–95, 1995–96, and 1996–97 seasons. http://www.cdc.gov/epo/mmwr/preview/mmwrhtml/ss4903a2.htm, April 2000. CDC compiled report for 1994-1997.

[3] G. Chowell, P. W. Fenimore, M. A. Castillo-Garsow, and C. Castillo-Chavez. Sars outbreaks in ontario, hong kong, and singapore: the role of diagnosis and isolation as a control mechanism. *Los Alamos Natl. Lab. Report*, 2003.

[4] A.L. Frank and L.H. Taber. Variation in frequency of natural reinfection with influenza-a viruses. *Journal Of Medical Virology*, 12(1):17–23, 1983.

[5] Lori Hutwagner. Telephone conversation about 122 cities mortality reporting system. Ms. Hutwagner works at the CDC Epidemiology Program, June 2001.

[6] J.M. Hyman and T. LaForce. Multi-city sir epidemic model. *Los Alamos Report*, 2001.

[7] J.M. Hyman and J. Li. An intuitive formulation for the reproductive number for the spread of diseases in heterogeneous populations. *Mathematical Biosciences*, 167(1):65 – 86, September 2000.

[8] I.M. Longini. A mathematical-model for predicting the geographic spread of new infectious agents. *Mathematical Biosciences*, 90(1-2):367 – 383, 1988.

[9] Denis Mollison, editor. *Epidemic Models: Their Structure and Relation to Data*. Cambridge University Press, 1995.

[10] Arnold S. Monto, James S. Koopman, and Ira M. Longini, Jr. Tecumseh study of illness XIII: Influenza infection and disease. *American Journal of Epidemiology*, 121(6):811–822, 1985.

[11] Office of the Assistant Secretary for Aviation and International Affairs. Domestic airline fares consumer report: Third quarter 1999 passenger and fare information. http://ostpxweb.dot.gov/aviation/domfares/993web.pdf, May 2000. Flight stats.

[12] L.A. Rvachev and I.M. Longini. A mathematical-model for the global spread of influenza. *Mathematical Biosciences*, 75(1):3 – 23, 1985.

[13] L. Sattenspiel and C.P. Simon. The spread and persistence of infectious-diseases in structured populations. *Mathematical Biosciences*, 90(1-2):341 – 366, 1988.

[14] N.I. Stilianakis, A.S. Perelson, and F.G. Hayden. Emergence of drug resistance during an influenza epidemic: Insights from a mathematical model. *Journal Of Infectious Diseases*, 177(4):863 – 873, April 1998.

[15] S.B. Thacker. The persistence of influenza a in human-populations. *Epidemiologic Reviews*, 8:129 – 142, 1986.

[16] Census 2000 PHC-T-3 ranking tables for metropolitan areas 1990 and 2000. http://blue.census.gov/population/cen2000/phc-t3/tab01.pdf, April 2001. table of populations according to 2001 census.

[17] Update: Influenza activity – United States and worldwide, 1997-98 season, and composition of the 1998-99 influenza vaccine. http://www.cdc.gov/mmwr/preview/mmwrhtml/00052002.htm, April 1998. CDC comiled report for 1997-1998.

[18] Update: Influenza activity — United States and worldwide, 1999–2000 season, and composition of the 2000–01 influenza vaccine. http://www.cdc.gov/epo/mmwr/preview/mmwrhtml/mm4917a5.htm, 1999. CDC compiled report for 1999-2000.

[19] Update: Influenza activity - United States and worldwide, 1998-99 season, and composition of the 1999-2000 influenza vaccine. http://www.cdc.gov/mmwr/preview/mmwrhtml/mm4818a2.htm, 1999. CDC compiled report for 1998-1999.

[20] Update: Influenza activity — United States and worldwide, 2000–01 season, and composition of the 2001–02 influenza vaccine. http://www.cdc.gov/mmwr/preview/mmwrhtml/mm5022a4.htm, 2001. CDC compiled report for 2000-2001.